Aalborg Universitet

Analysis of Harmonic Coupling and Stability in Back-to-Back Converter Systems for Wind Turbines using Harmonic State Space (HSS)

Kwon, Jun Bum; Wang, Xiongfei; Bak, Claus Leth; Blaabjerg, Frede

Published in:
Proceedings of the 2015 IEEE Energy Conversion Congress and Exposition (ECCE)

DOI (link to publication from Publisher):
10.1109/ECCE.2015.7309762

Publication date:
2015

Document Version
Accepted author manuscript, peer reviewed version

Link to publication from Aalborg University

Citation for published version (APA):
Kwon, J. B., Wang, X., Bak, C. L., & Blaabjerg, F. (2015). Analysis of Harmonic Coupling and Stability in Back-to-Back Converter Systems for Wind Turbines using Harmonic State Space (HSS). In *Proceedings of the 2015 IEEE Energy Conversion Congress and Exposition (ECCE)* (pp. 730-737). IEEE Press.
https://doi.org/10.1109/ECCE.2015.7309762

General rights
Copyright and moral rights for the publications made accessible in the public portal are retained by the authors and/or other copyright owners and it is a condition of accessing publications that users recognise and abide by the legal requirements associated with these rights.

- Users may download and print one copy of any publication from the public portal for the purpose of private study or research.
- You may not further distribute the material or use it for any profit-making activity or commercial gain
- You may freely distribute the URL identifying the publication in the public portal -

Take down policy
If you believe that this document breaches copyright please contact us at vbn@aub.aau.dk providing details, and we will remove access to the work immediately and investigate your claim.

Downloaded from vbn.aau.dk on: December 05, 2025

Analysis of Harmonic Coupling and Stability in Back-to-Back Converter Systems for Wind Turbines using Harmonic State Space (HSS)

JunBum Kwon, Xiongfei Wang, Claus Leth Bak, Frede Blaabjerg
Department of Energy Technology
Aalborg University
Aalborg, Denmark
E-mail : jbk, xwa, clb, fbl @et.aau.dk

Abstract – Understanding about harmonic propagation in wind turbine converter is fundamental to research the influence of these on a large network harmonic distortion. Therefore, the analysis of wind turbine converter harmonic spectrum as well as the influence of converter operating point into the network is urgently important issues in harmonic studies on wind farm. However, the conventional modeling procedure and simplified model for controller design are not enough to analyze such complicated systems. Besides, they have many limitations in terms of including a non-linear component, different operating points and harmonic coupling analysis. Hence, it is critically needed to develop the advanced converter model, which can include almost all the possibilities. This paper develops the advanced Back to Back (BtB) converter model for wind farm application by means of Harmonic State Space (HSS) modeling method. The modeling and analysis results are remarkable that this model can include non-linear component and also show different operating points and harmonic coupling point, where this means each wind power converter can show the different impedance characteristics. The developed model can easily connected into the large wind farm model to analyze the overall steady-state harmonic as well as harmonic stability. All theoretical modeling and analysis is verified by means of simulation and experimental results.

Keywords—Harmonic State Space Modeling, Wind-turbine, Back-to-Back Converter, Harmonic instability, Harmonics coupling

I. INTRODUCTION

The number of wind turbine used in offshore wind farm is rapidly increasing. Among them, most of their topology is now changing to back-to-back converter type in order to get more flexible controllability and to meet the grid code [1]. However, both steady-state harmonic coupling and dynamic harmonic interaction in the back-to-back converter is challenging the power quality of wind turbines. There is an urgent need to find an analytical way to map the source of harmonics and instabilities [2]. As all wind turbine back-to-back converters connected through a submarine cable with a large capacitance. Besides, each wind turbine in wind farm is working at different operating point because of the wind direction and control strategy. Furthermore, the non-linearity and complexity of wind farm make analysis difficult for such system. Consequently, these operation can change the wind farm`s internal impedance, continuously [3, 4]. As a result, a large wind farm can affect to the other wind farms connected MV or HV network through an unpredicted harmonic coupling or a resonance problem. Hence, an accurate analysis method of the complex system is becoming more important.

In order to design the controller and to analyze the response of the impedance of a power converter at a specific operating point, a linearized state-space averaging method has been widely used [5]. However, it has limitation in the analysis of the power converter, which is having a low switching frequency characteristic. Besides, the usage is very limited in case of multi connected system and coupling analysis. Typically, FFT and Wavelet analysis methods are practically used in the field for the analysis harmonics, which is changing according to the time, and also used to steady-state harmonic. From these results, probabilistic approaches are also used to know the density of harmonic in time and frequency scale [6] . However, they are difficult to use in the analysis of impedance coupling as well as their relationship.

To overcome this challenge and limitation, new approaches, which are reflecting the time varying signal properties, are introduced [7-9]. The Harmonic State Space (HSS) modeling method is introduced in power system studies [10] in order to show a more complete harmonic impedance coupling. Based on the theory of Harmonic Domain (HD) [11], Extended Harmonic Domain (EHD) [12], and Harmonic Transfer Function (HTF) [13], the HSS modeling method is developed to analyze the harmonic coupling and also the stability with the additional harmonic impedance.

This paper presents a harmonic coupling analysis of a back-to-backwind turbine converter. First, each PWM converter is modeled using the HSS modeling approach. Then, a combined model is described using a linearization procedure. In order to concentrate the harmonic instability analysis of a full-scale converter, the generator is simplified into a simple filter. Second, the steady-state harmonic coupling between two converters is analyzed according to the variation of the wind-turbine speed. Consequently, the modeling approach and analyzed results show that each harmonic is coupled with each other according to the operation of the wind turbine. Furthermore, the derived results show different impedance characteristic with traditional linearized model. The analyzed

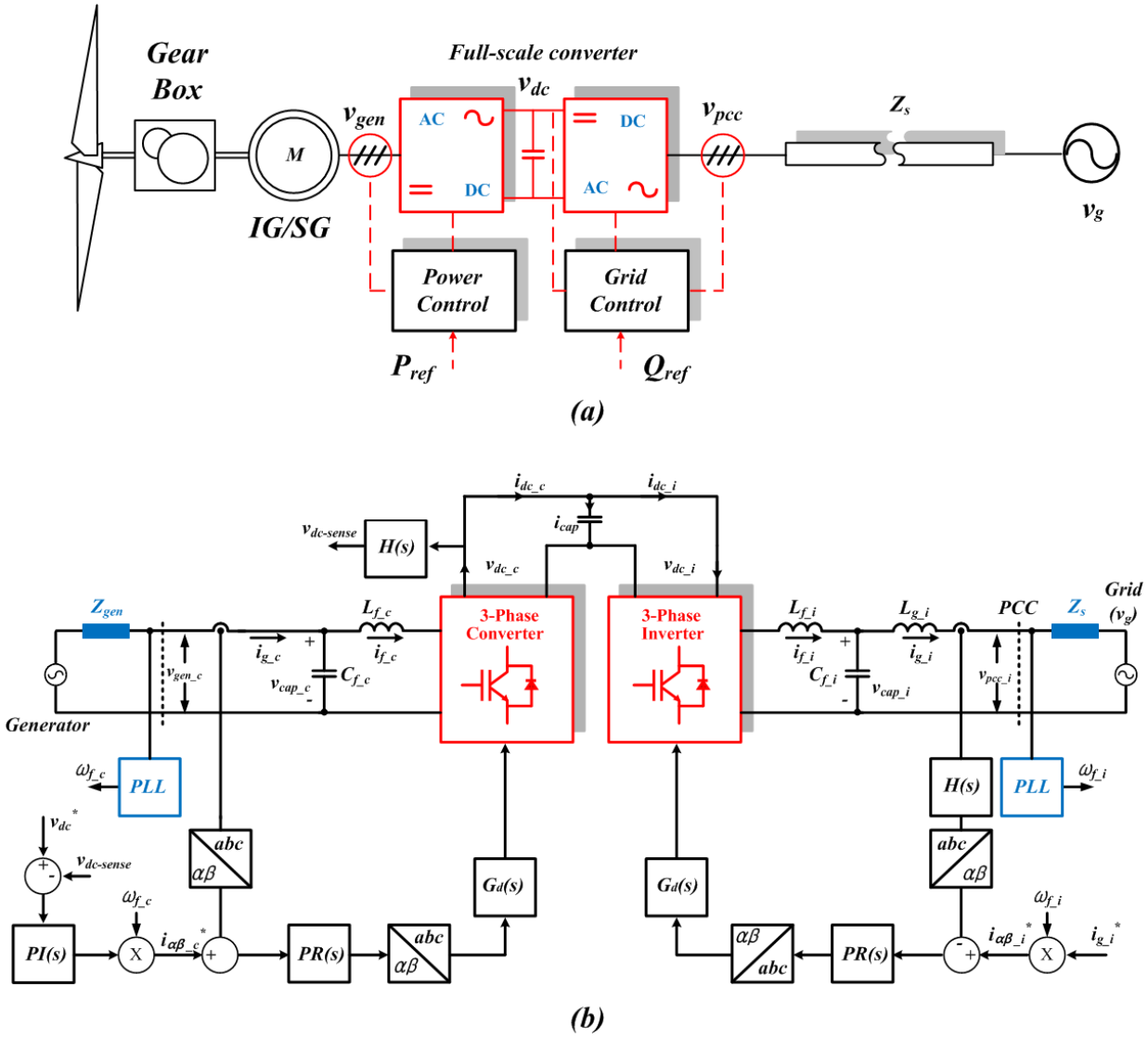

Fig. 1. Block diagram for Full-scale back to back (BtB) converter
(a) Structure of wind turbine converter (b) Block diagram of the simplified model

results are fully verified by time-domain and the frequency-domain simulation as well as experimental results.

II. HSS Modeling Of Wind Turbine Full-Scale Converter

A. System Description

Single Wind Turbine Converter (WTC) is considered for the modeling as shown in Fig. 1-(a). Even though the Induction Generator (IG) or Synchronous Generator (SG) can be taken into account as the generator, the generator is simplified as the large inductance ($Z_{gen} = L_{g\_c}+R_{g\_c}$) in order to focus on the harmonics driven by the input frequency. The effect of gear box is also not considered in the model, where the frequency of RSC is assumed as from 2 Hz ~ 20 Hz. Furthermore, the motor side controllers including the Maximum Power Point Tracking (MPPT) are simplified to the algorithm for the grid connected converter as shown in Fig. 1-(b). To synchronize with the rotor side frequency, PLL is used with the Proportional Resonant (PR) Controller. In case of GSC, the PLL is also considered to synchronize with the grid frequency. Additionally, the dc link voltage is governed by the dc voltage controller in RSC as shown in Fig. 1-(b). The detail system parameter for the modeling and simulation are given by Table I.

B. Review of HSS modeling

In LTI model, it is difficult to analyze the full-scale dynamics as well as their relation because the dynamics in dc circuit. Besides, the impedance characteristics derived from LTI model can only show a fundamental frequency components. It will just show the response about the variation of input magnitude and phase delay. However, almost all important parameters, i.e non-linear inductor, modulation index, dc-harmonic, are varying according to the system operation, which means that the response of other frequency component is critically important information in complex

Table I. System parameter

Conv.	P_{rate}	L_f (mH)	R_{Lf} (mΩ)	C_f (uF)	R_{Cf} (mΩ)	L_g (mH)	R_{Lg} (mΩ)	V_{dc} (V)	C_{dc} (uF)	R_{dc} (Ω)	f_{sw} (kHz)
RSC	35kVA	0.87	11.4	22	7.5	0.22	2.9	750	1000	10	2
GSC	35kVA	1.2	15.7	15	11	03	3.9	750	1000	10	2

electrical system. Hence, the Linear Time Varying (LTV) system is also considerable in terms of steady-state as well as dynamic performance of a large system. Practically, these were challenge to be solved in the traditional way. However, if all signals are assumed to be varying periodically, it is possible to linearize by means of Fourier series [14]. Based on these assumption and definition, the HSS model can have a format as shown in (1), where X_n is harmonic state matrix, Y_n is output harmonic matrix, U_m is input harmonic matrix and A_{n-m} is harmonic state transition matrix driven from the LTP theory [15]. $B_{n-m}, C_{n-m}, D_{n-m}$ are also a harmonic state matrix analogously, which is dependent on the number of input and output. All the matrix size is dependent on the number of harmonics considered in the HSS modeling procedure. In this paper, "+40th ~-40th" harmonic are considered in order to see the harmonic coupling by the 40th harmonic, where this is based on the assumption that the harmonics above 2 kHz are out of interest because of control bandwidth.

$$(s + jm\omega_0)X_n = \sum_{-\infty}^{\infty} A_{n-m}X_m + \sum_{-\infty}^{\infty} B_{n-m}U_m \qquad (1)$$
$$Y_n = \sum_{-\infty}^{\infty} C_{n-m}X_m + \sum_{-\infty}^{\infty} D_{n-m}U_m$$

C. HSS modeling of RSC topology

Based on (1), a 3-phase grid connected PWM converter and inverter are modeled according to the procedure described in [16]. The modeling results of one converter are shown in (2), where, "*I*" means the identity matrix and "*N*" is the dynamic matrix, which is derived from (1). The time domain switching function is reorganized into a Toeplitz (Γ) [17] matrix in order to perform a convolution by means of the method described in Fig. 1. The small letter in Fig. 1 means the time domain signal. On the other hand, the capital letters in (2) stand for the harmonic coefficient component, which is derived from the Fourier series.

Based on (2), the final block diagram of the single 3-phase grid connected PWM converter is drawn in Fig. 2. The harmonic coefficient vector from the generator ($V_{gen\_c-abc(-h\ldots h)}$) is transferred into the LCL-filter side harmonic transfer function. The calculated harmonic vector of the inverter side filter current ($I_{f\_c-abc(-h\ldots h)}$) is transferred into the dc-side harmonic transfer function through a linearized switching harmonic vector ($\Gamma[SW_C]$). The summation of each phase current ($I_{g\_c-ABC(-h\ldots h)}$) is dc current harmonic vector ($I_{dc\_c(-h\ldots h)}$), where this is convoluted with the dc network harmonic vector (C_{dc}) in order to get a dc voltage harmonic vector ($V_{dc1(-h\ldots h)}$). The results are convoluted again with the switching harmonic vector ($\Gamma[SW_C]$)

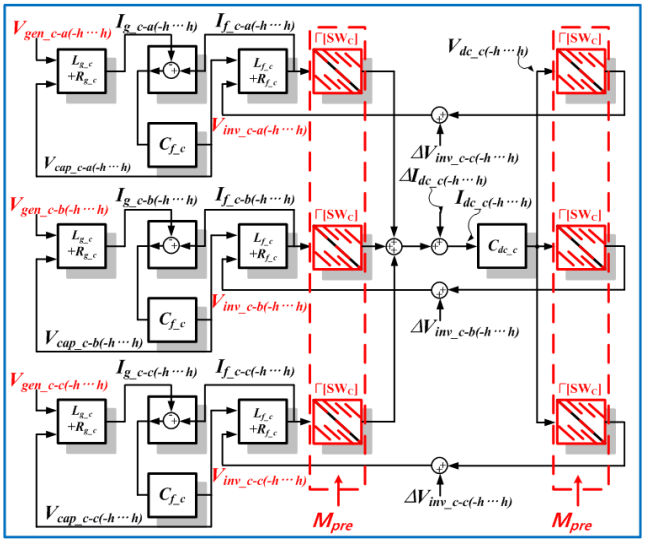

Fig. 2. Block diagram for the HSS modeling of RSC and GSC topology

in order to obtain the harmonic vector of the inverter side voltage ($V_{inv\_c-abc(-h\ldots h)}$). The derived harmonic vector of converter side voltage is transferred to the LCL filter side harmonic transfer function, repetitively, in order to get the response of each harmonic vector. Conclusively, the linearized switching harmonic vector ($\Gamma[SW_C]$), which is decide by the previous modulation (M_{Pre}), governs the voltage and current data at the previous steady state. However, the small variation (Δ) should be added to the nominal values, which are obtained from the calculation or the previous state, in order to obtain the dynamic response. Thus, these small variations ($\Delta V_{inv\_c-abc}, \Delta I_{dc\_c}$) can be updated from the controller.

$$\begin{bmatrix} \dot{I}_{g\_c-abc}(t) \\ \dot{I}_{f\_c-abc}(t) \\ \dot{V}_{cap\_c-abc}(t) \\ \dot{V}_{dc\_c}(t) \end{bmatrix} = \begin{bmatrix} \frac{-R_{g\_c}}{L_{g\_c}}I - N & 0 & \frac{-1}{L_{g\_c}}I & 0 \\ 0 & \frac{-R_{f\_c}}{L_{f\_c}}I - N & \frac{1}{L_{f\_c}}I & -\frac{\Gamma[SW^T]}{L_f} \\ \frac{1}{C_{f\_c}}I & \frac{-1}{C_{f\_c}}I & -N & 0 \\ 0 & \frac{\Gamma[SW]}{C_{dc\_c}} & 0 & -N \end{bmatrix} \begin{bmatrix} I_{g\_c-abc}(t) \\ I_{f\_c-abc}(t) \\ V_{cap\_c-abc}(t) \\ V_{dc\_c}(t) \end{bmatrix} + \begin{bmatrix} \frac{1}{L_{g\_c}}I \\ 0 \\ 0 \\ 0 \end{bmatrix} [V_{gen\_c-abc}(t)] \qquad (2)$$

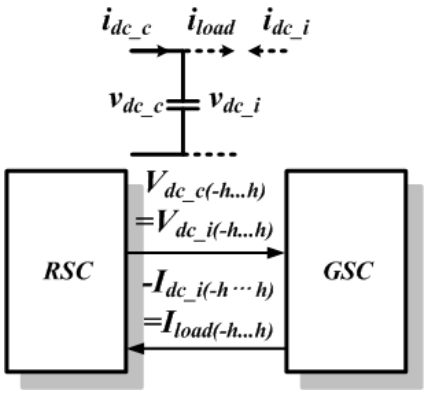

Fig. 3. Exchange of harmonic vector information between RSC and GSC

D. HSS mode ling of GSC topology

The topology of the GSC can also be modeled by means of the similar way with the RSC. However, another harmonic flow should be considered to combine the RSC and GSC at a one domain. The dc link circuit of the full-scale converter can be modeled by changing the plus sign (+) of dc current in GSC side ($I_{dc\_i(-h...h)}$) into the minus (-) sign. Hence, the harmonics vector of the reversed GSC dc current ($I_{dc\_i(-h...h)}$) can be regarded as the load current of the RSC ($I_{load(-h...h)}$). As a result, the structure of the two (GSC, RSC) blocks can be connected as shown in Fig. 3. The exchange of harmonics vector between RSC and GSC can make it possible to explain the harmonics coupling, which is generated from the RSC to the GSC.

Based on the result from the topology model, the controller can be added to each model, where the PI, PR controller are mainly used for the control of dc link voltage, generator side current and the grid side current. The detail procedure for the controller modeling is performed by [16].

III. Simulation And Experimental Results

In order to verify the modeling and analysis of the back to back converters, MATLAB and PLECS are used for time and frequency domain simulation in order to study the two different assessment methods. Laboratory tests are also performed on an experimental set-up, where two 3-phase frequency converters are connected to compose a back to back converter. The control algorithms are implemented in a DS1007 dSPACE system in order to see the harmonic components. In order to consider the harmonics below 2 kHz, the number of harmonics for the HSS modeling are considered from -40th to 40th order.

A. Flowchart for the simulation

To validate the developed HSS model with the simulation in the switch model, the flowchart in Fig. 4 is used. The overall sequence is as follows:

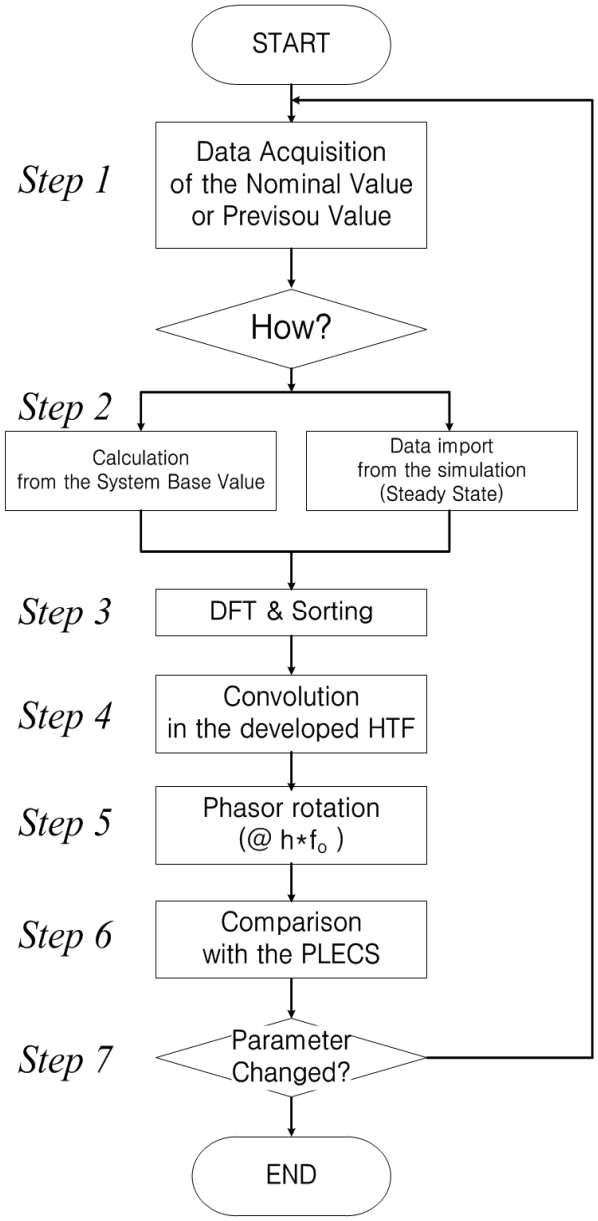

Fig. 4. Flowchart for the validation of HSS model with the nonlinear time domain simulation

Step 1) It is required to obtain the main waveform, for instance, the grid current, grid voltage, and the converter voltage, etc, which can be the system nominal value or the previous state.

Step2) Two methods can be chosen according to the complexity of the system. If the main data can be calculated from the base value of power rating and voltage, the nominal data can be easily acquired by using the calculation. On the contrary, if the system is complex, the important data can directly be measured from the time domain simulation.

Step3) Based on the steady state value, the data can be transformed into the frequency information by means of the Discrete Fourier Transform (DFT). After then, the Fourier coefficient can be sorted and rearranged in order to be

matched with the harmonic sequence of the developed the HSS model.

Step4) The rearranged data can be the base valued of the HSS model. Therefore, the output harmonic vectors can be calculated by using the convolution with the HTF.

Step5) The derived output harmonics can be converted into the time domain data through the phasor rotation at a specific frequency ($h \cdot f_o$), where h is the harmonic number and the f_o is the fundamental frequency concerned.

Step6) The converted time domain waveforms can be compared with the nonlinear time domain simulation to verify the HSS model.

Step7) If the main parameters are changed to test the dynamics, the HTF should be calculated again based on the previous nominal values. Because the model obtained at the first time means the operating condition at that moment. Hence, the HTF should be calculated and checked again when the system operating point is changed.

B. Steady-state and Dynamic performance

According to the modeling results in Section II, the HSS model of the back-to-back converter can be converted into a harmonic transfer function [18] by means of "$H_k(s) = \sum_l \hat{C}_{k-l}\left((s + jl\omega_0)I - \hat{A}\right)^{-1}\hat{B}_l + D_k$". Each harmonic frequency response from Harmonic Transfer Function (HTF) can be converted into time domain by rotating a phasor at a specific harmonic frequency. The noticeable characteristic of harmonic transfer function is that "$H_0(s)$"is the same with the LTI model frequency response characteristic. Hence, the LTP model, which is including other harmonic frequency responses in a single coordinate, can show more precise response than the LTI model. The derived HTF can be simulated according to the procedure given in Fig. 4.

At first a 50 Hz frequency on both RSC and GSC sides are considered as a case to verify the validity of the HSS modeling results. All input, output and state variable are Fourier coefficients, which mean that each signal is composed by harmonic components. The final derived results from the HTF are shown in Fig. 5, where two case studies are performed to investigate the dynamic response of the HSS model. The rotor side current is decided by the dc voltage reference. Additionally, the grid side current is controlled by the current controller of GSC. As shown in Fig 5, the steady state results are well controlled by the HSS controller. The dynamic status is also well converged at 0.5 sec, when the dc voltage reference is changed from 750 V to 700 V. It can be found that the RSC side ac current (I_{g_c}) is reduced and the dc voltage is also converged into the changed reference. However, the GSC side ac current (I_{g_i}) are tracing the current reference value again as shown in Fig. 5-(a). As a second case, the reference for the GSC side ac current (I_{g_i}) is changed from 10 A to 20A. The rotor side current (I_{g_c}) is also increased due to the same input and output power. Furthermore, both the rotor side dc current (I_{dc_c}) and the grid side dc current (I_{dc_i}) are also increased simultaneously. However, the dc voltage (V_{dc}) keeps the reference voltage with the dynamic variation.

To analyze how each HTF are coupled in frequency response, the closed loop transfer functions are drawn as an example in Fig. 5-(c), (d), where I_{g_i}/V_{g_c} is drawn with two cases. For the visibility, 11th order harmonics are only considered in Fig. 5-(c). It can be found that the 0 frequency and 2nd / -2nd order harmonics are strongly coupled than the other HTF, which means the 0~600 Hz input will be affected by the 0, -2, 2 order HTF. Furthermore, the +/- 1st order HTF are coupled to the admittance response between RSC side input voltage and the dc voltage. As a result, the derived HTF model for the BtB conveter can show how the frequency is coupled each other, where the other HTF response has also the possibility to be important than the HTF according to the connected device, when the system is becoming complex.

Based on this modeling result, the harmonic frequency can also be divided into more precise frequency components in order to consider the varying input frequency of the rotor side converter. For example, a fundamental frequency (f_o) or harmonic frequency (f_h) can be divided by specific frequencies. In this paper 5 Hz is used as the base frequency (f_b) of harmonic components (-40th ~40th), which means the each signal is decomposed by a 5 Hz frequency unit as shown in (3).

$$\frac{f_o}{f_b} = m \quad , \qquad \frac{f_h}{f_b} = n \tag{3}$$

The "m" means the row or column matrix number of the matrix for fundamental frequency. Similarly, "n" means the row or column number of matrix for harmonic frequency. For instance, m is 10 if fundamental frequency (f_o) is 50Hz and base frequency (f_b) is 5Hz, where fundamental harmonic is located in the 10th row and column side of matrix. When increasing the number of used harmonics in the modeling, the size of matrix will be increased. However, the calculation time of a large matrix can be reduced by means of using sparse matrix [11]. The simulation results and the frequency response with two different frequencies are shown in Fig. 6, where the frequency of RSC is 10 Hz and the GSC is 50Hz are applied to analyze the frequency coupling. Similarly to the 50 / 50 Hz case, the same transient simulations are performed to validate the HSS model. Furthermore, the different HTF can be found compared to the HTF in Fig. 5, where the HTF in Fig. 6 has low admittance in 10 Hz and the different frequency response in other frequency range. This means that the HTF are coupled by the frequency response of 10 Hz as shown in Fig. 6. It is noticeable that the input frequency and magnitude affect to the frequency response of the BtB converter, where it can not be explained in the LTI model.

The experimental results are also compared with the simulation results as shown in Fig. 7, which is obtained by the same procedure with Fig. 4. They matched well the PLECS simulation results as shown in Fig. 7-(b). This means that the HTF is able to model the coupled harmonics. Furthermore, the simulations are compared with the experimental results as shown in Fig. 7-(a). Even though the compared results are well matched, it contains the small errors, which is driven by the dead time and the error in FFT. This can be improved by increasing the number of harmonics and time step.

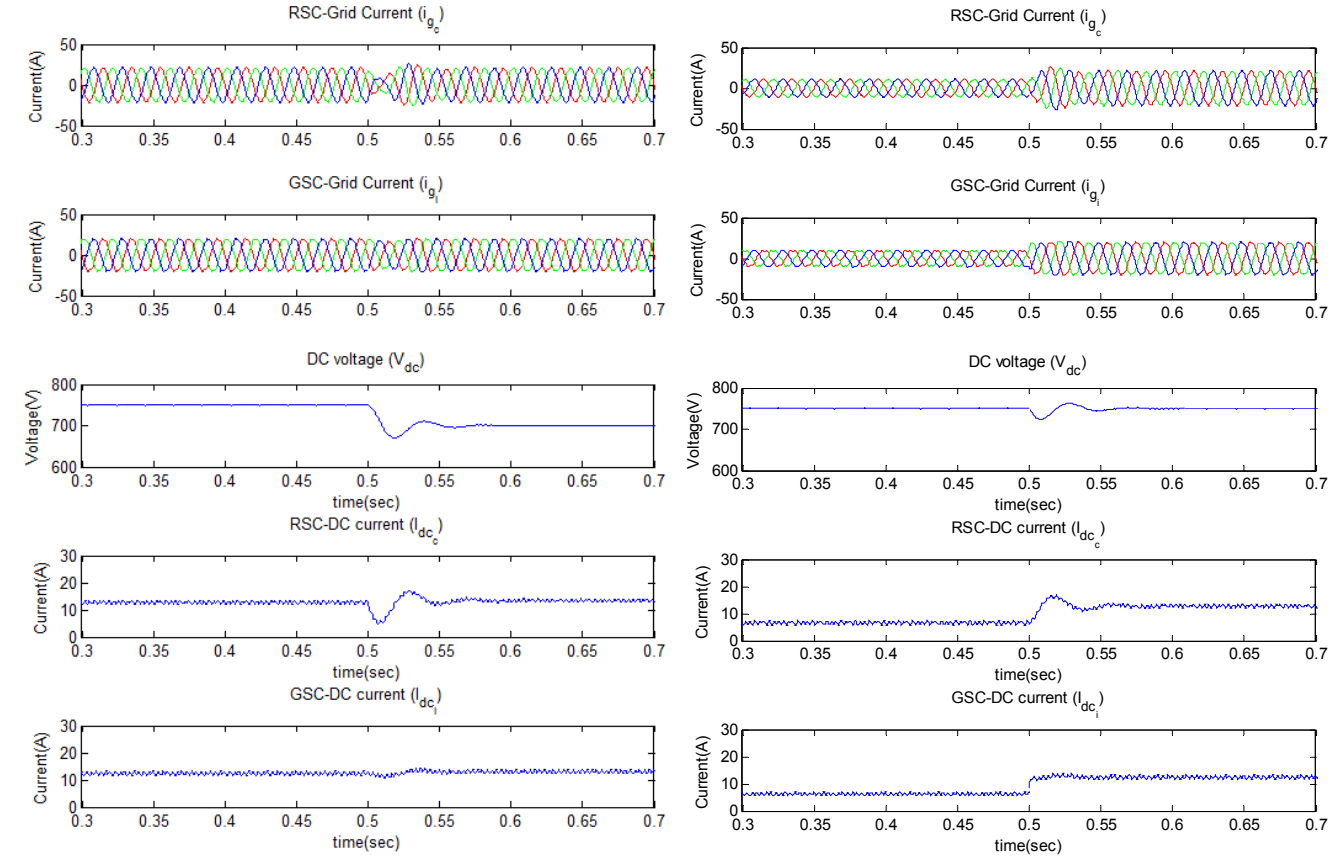

(a) (b)

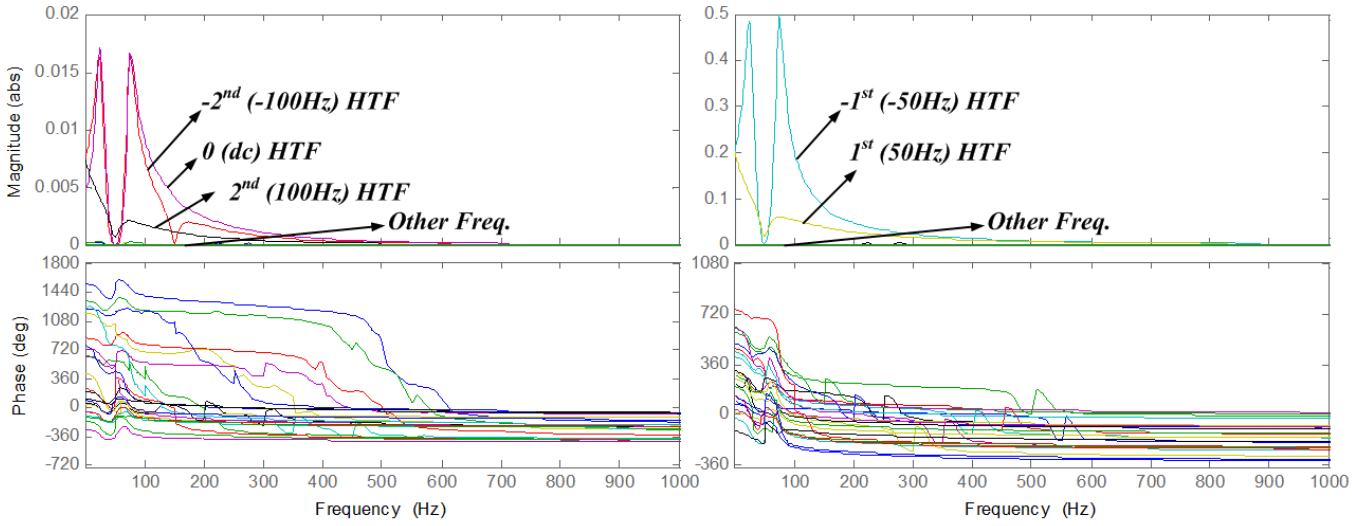

(c) (d)

Fig. 5. Time domain simulation result and the HTF (RSC=50Hz, GSC=50Hz)

(a) DC voltage reference variation at 0.5 sec, (b) Grid current reference variation at 0.5 sec, (c) Admittance response (RSC side input voltage (Phase A) to GSC side grid current (Phase A)), when the harmonics (-11th~11th) are considered, (d) Admittance response (RSC side input voltage (Phase A) to DC link voltage), when the harmonics (-11th~11th) are considered.

IV. Con clusion

This paper proposes a new back to back converter model using the HSS modeling approach for the analysis of harmonic instability. The simulation results derived from the HSS modeling as well as the experimental results show the same waveforms with a non-linear time domain simulation results. The remarkable difference among them is that HSS modeling

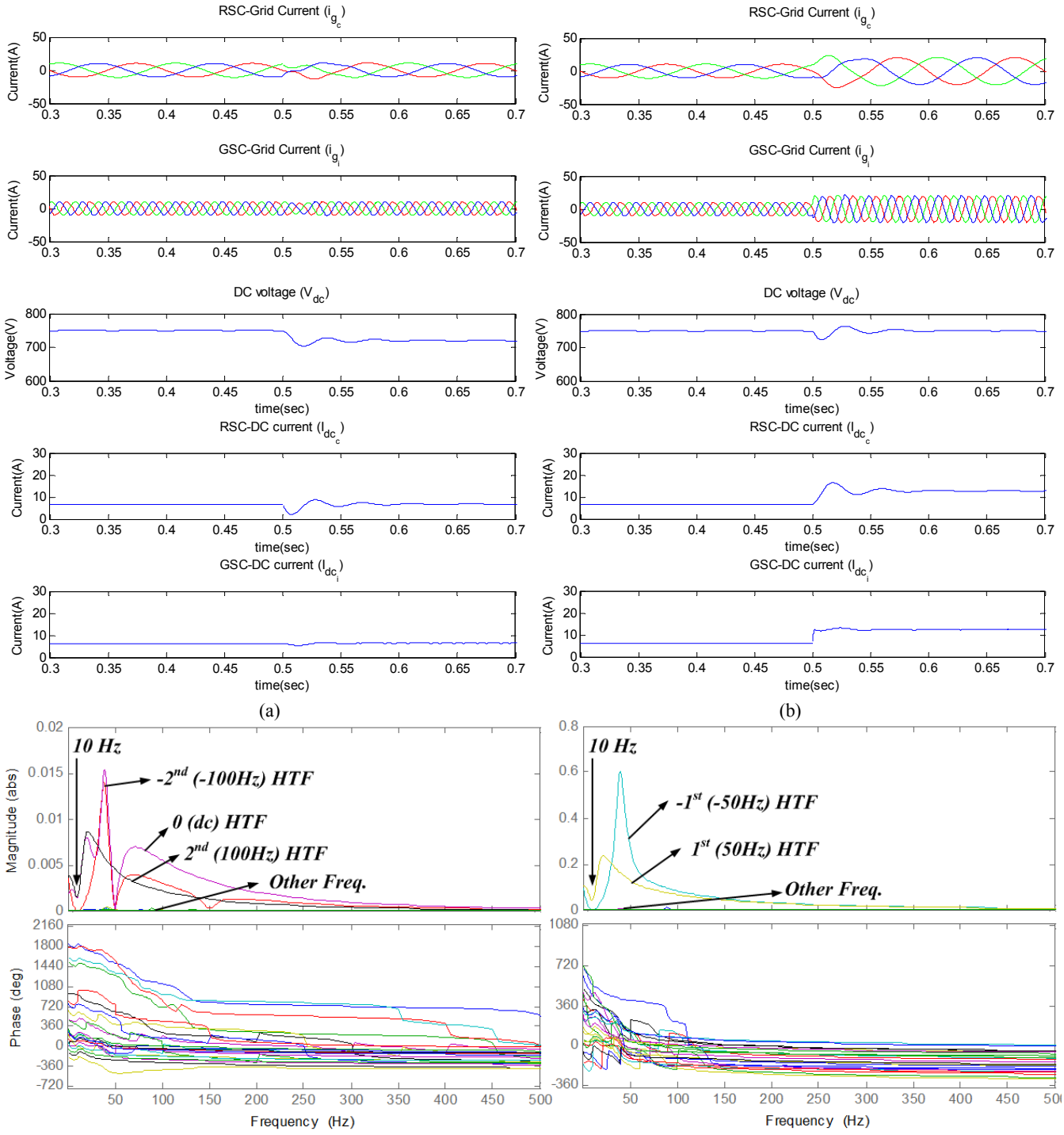

Fig. 6. Time domain simulation result and the HTF (RSC=10Hz, GSC=50Hz)

(a) DC voltage reference variation at 0.5 sec, (b) Grid current reference variation at 0.5 sec, (c) Admittance response (RSC side input voltage (Phase A) to GSC side grid current (Phase A)), when the harmonics (-11^{th}~11^{th}) are considered, (d) Admittance response (RSC side input voltage (Phase A) to DC link voltage), when the harmonics (-11^{th}~11^{th}) are considered.

is a linearized model with the number of harmonics. Furthermore, the HSS model can show different harmonic impedance information which can be used in the analysis of harmonic coupling. Furthermore, the response of the HSS model from a single frequency input is the multiple frequency output. Hence, it can represent the coupling characteristics between the BtB converters in one domain, where the traditional LTI approach can not show this characteristic simultaneously.

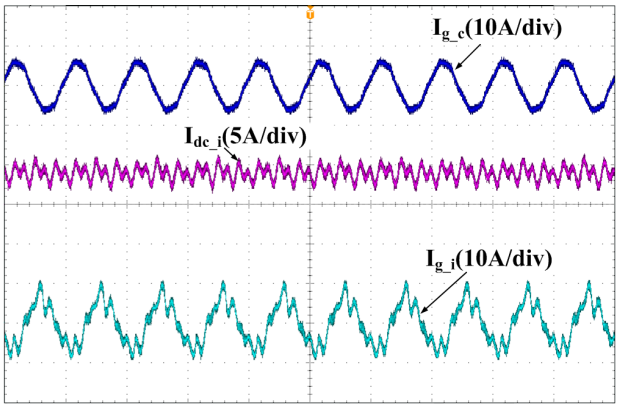

(a)

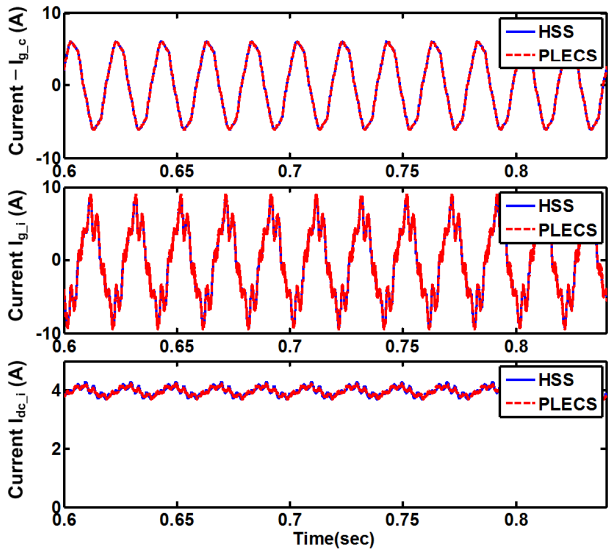

(b)

Fig 7. Simulation and experimental results at 3 kW power rating using HSS modeling and PLECS
RSC : L_{gen} = 620 uH, L_{fc} = 1.7 mH, C_{fc} = 6 uF, $C_{dc\text{-}c}$ = 1000 uF, $V_{in(line\text{-}line)}$ = 380 V, switching frequency = 6 kHz
GSC : L_{fi} = 3 mH, L_{gi} = 1 mH, C_{fi} = 4.7uF, $C_{dc\text{-}i}$ = 1000 uF, $V_{pcc(line\text{-}line)}$ = 380 V, switching frequency = 10 kHz
- Grid side inductor current simulation (harmonic = -40^{th} ~40^{th})
waveform (a) Experimental results (blue = grid side current ($\mathbf{I_{g\_i}}$), cyan= converter side current ($\mathbf{I_{g\_c}}$), purple = dc current ($\mathbf{I_{dc\_i}}$))
(b) Simulation results (grid side current ($\mathbf{I_{g\_i}}$), converter side current ($\mathbf{I_{g\_c}}$), dc current ($\mathbf{I_{dc\_i}}$))

ACKNOWLEDGMENT

This work was supported by European Research Council under the European Union's Seventh Framework Program (FP/2007-2013)/ERC Grant Agreement n. [321149-Harmony]

REFERENCES

[1] R. Teodorescu and F. Blaabjerg, "Flexible control of small wind turbines with grid failure detection operating in stand-alone and grid-connected mode," *IEEE Trans. Power Electron.,* vol. 19, pp. 1323-1332, 2004.

[2] X. Wang, F. Blaabjerg, and W. Weimin, "Modeling and Analysis of Harmonic Stability in an AC Power-Electronics-Based Power System," *IEEE Trans. on Power Electron.,* vol. 29, pp. 6421-6432, 2014.

[3] M. Bollen, J. Meyer, H. Amaris, A. M. Blanco, A. Gil de Castro, J. Desmet*, et al.*, "Future work on harmonics - some expert opinions Part I - wind and solar power," in *Proc. IEEE ICHQP*, 2014, pp. 904-908.

[4] J. Meyer, M. Bollen, H. Amaris, A. M. Blanco, A. Gil de Castro, J. Desmet*, et al.*, "Future work on harmonics - some expert opinions Part II - supraharmonics, standards and measurements," in *Proc. IEEE ICHQP*, 2014, pp. 909-913.

[5] A. Emadi, "Modeling and analysis of multiconverter DC power electronic systems using the generalized state-space averaging method," *IEEE Trans. Ind. Electron.,* vol. 51, pp. 661-668, 2004.

[6] L. Sainz, J. J. Mesas, R. Teodorescu, and P. Rodriguez, "Deterministic and Stochastic Study of Wind Farm Harmonic Currents," *IEEE Trans. Energy Conv.,* vol. 25, pp. 1071-1080, 2010.

[7] B. Jing, L. Hong, and T. Q. Zheng, "Stability analysis of grid-connected inverters with LCL-filter based on harmonic balance and Floquet theory," in *2014 International Proceeding on Power Electronics Conference (IPEC-Hiroshima 2014 - ECCE-ASIA),* , 2014, pp. 3314-3319.

[8] W. Faqiang, Z. Hao, and M. Xikui, "Analysis of Slow-Scale Instability in Boost PFC Converter Using the Method of Harmonic Balance and Floquet Theory," *IEEE Trans. on Circuits and Systems,* vol. 57, pp. 405-414, 2010.

[9] W. Xiaoqun, W. Siu-Chung, C. K. Tse, and L. Junan, "Bifurcation Behavior of SPICE Simulations of Switching Converters: A Systematic Analysis of Erroneous Results," *IEEE Trans. Power Electron.,* vol. 22, pp. 1743-1752, 2007.

[10] M. S. P. Hwang and A. R. Wood, "A new modelling framework for power supply networks with converter based loads and generators - the Harmonic State-Space," in *Proc. of IEEE POWERCON*, 2012, pp. 1-6.

[11] J. Arrillaga and N. R. Watson, "The Harmonic Domain revisited," in *Proc. of IEEE ICHQP*, 2008, pp. 1-9.

[12] J. J. Rico, M. Madrigal, and E. Acha, "Dynamic harmonic evolution using the extended harmonic domain," *IEEE Trans. Power Deliv.,* vol. 18, pp. 587-594, 2003.

[13] E. Mollerstedt and B. Bernhardsson, "Out of control because of harmonics-an analysis of the harmonic response of an inverter locomotive," *IEEE Trans. on Control Sys.,* vol. 20, pp. 70-81, 2000.

[14] N. M. Wereley and S. R. Hall, "Frequency response of linear time periodic systems," in *Proc. of IEEE CDC*, 1990, pp. 3650-3655 vol.6.

[15] N. M. Wereley and S. R. Hall, "Linear Time Periodic Systems: Transfer Function, Poles, Transmission Zeroes and Directional Properties," in *Proc. of IEEE ACC*, 1991, pp. 1179-1184.

[16] J. Kwon, X. Wang, C. L. Bak, and F. Blaabjerg, "Harmonic Interaction Analysis in Grid Connected Converter using Harmonic State Space (HSS) Modeling," in *Proc. IEEE APEC 2015*.

[17] J. R. C. Orillaza and A. R. Wood, "Harmonic State-Space Model of a Controlled TCR," *IEEE Trans. Power Deliv.,* vol. 28, pp. 197-205, 2013.

[18] H. Sandberg, E. Mollerstedt, and Bernhardsson, "Frequency-domain analysis of linear time-periodic systems," *IEEE Trans. Auto. Control,* vol. 50, pp. 1971-1983, 2005.